ChemPubSoc Europe

DOI: 10.1002/cmdc.201500335

CHEMMEDCHEM Full Papers

Tetrazolylhydrazides as Selective Fragment-Like Inhibitors of the JumonjiC-Domain-Containing Histone Demethylase KDM4A

Nicole Rüger,[a] Martin Roatsch,[b] Thomas Emmrich,[a] Henriette Franz,[c] Roland Schüle,[c] Manfred Jung,[b] and Andreas Link*[a]

The JumonjiC-domain-containing histone demethylase 2A (JMJD2A, KDM4A) is a key player in the epigenetic regulation of gene expression. Previous publications have shown that both elevated and lowered enzyme levels are associated with certain types of cancer, and therefore the definite role of KDM4A in oncogenesis remains elusive. To identify a novel molecular starting point with favorable physicochemical properties for the investigation of the physiological role of KDM4A, we screened a number of molecules bearing an iron-chelating moiety by using two independent assays. In this way, we were able to identify 2-(1*H*-tetrazol-5-yl)acetohydrazide as a novel fragment-like lead structure with low relative molecular mass ($M_r = 142$ Da), low complexity, and an IC_{50} value of 46.6 μM in a formaldehyde dehydrogenase (FDH)-coupled assay and 2.4 μM in an antibody-based assay. Despite its small size, relative selectivity against two other demethylases could be demonstrated for this compound. This is the first example of a tetrazole group as a warhead in JMJD demethylases.

Introduction

The human enzyme lysine-specific demethylase 4A is encoded by the *KDM4A* gene,[1] a member of the Jumonji domain 2 (JMJD2/KDM4) subfamily (isoforms A–E).[2] Under non-pathological conditions, the expression of this gene in many normal tissues is low, but there is ample evidence that elevated KDM4A levels are associated with certain types of malignant neoplasms. The enzyme could be identified as integral to the proliferation of bladder,[3] colon,[4] lung,[5] and prostate cancers,[6] isolated breast cancer cell lines,[7] and also in manifest breast cancer.[8] Overexpression of KDM4A was demonstrated at the RNA level by real-time PCR, as well as at the protein level by immunohistochemical staining. Moreover, suppression of KDM4A expression in lung and bladder cancer cells resulted in significant suppression of cell growth in these experiments.[3] As expression levels of KDM4A were low in normal tissues in all aforementioned cases, specific inhibitors of this enzyme may have a decreased risk of adverse reactions.[9] In stark contrast, other investigations have shown that KDM4A levels were significantly lower in malignant urothelium tissue than in healthy tissue, which could also be associated with a negative prognosis.[10] At this point, the reader is referred to the extensive and in-depth reviews of KDM4A's complex role in cancer by Hoffmann et al.[9] and Guerra-Calderas et al.[11] While there seems to be a general trend regarding the correlation between elevated KDM4A expression levels and cancer, the opposite was observed as well. This picture is even further complicated by the influence of single-nucleotide polymorphisms within the *KDM4A* gene, as recently reported by Van Rechem et al.[12] Thus, the definite role of this enzyme in oncogenesis remains to be determined.

Structures of the catalytic-core domain of KDM4A with and without its natural substrate, 2-oxoglutarate (**1**), in the presence of Ni^{2+} have been determined by X-ray crystallography.[13] The structure of the core domain, consisting of the JmjN domain, the JmjC domain, the C-terminal domain, and a zinc finger motif, revealed the unique elements that form a potential substrate binding pocket.[14] In addition, the enzyme features a JD2H domain, two TUDOR domains, and another PHD-type zinc finger,[15] which have not yet been resolved crystallographically. This nuclear protein functions as 2-oxoglutarate- and Fe^{II}-dependent oxygenase, which catalyzes a diverse set of reactions.[16] In vitro, KDM4A specifically demethylates di- and trimethylated residues of lysine 9 and 36 of histone H3 (H3K9/36$me_{2/3}$)[17] through initial hydroxylation of the *N*-(ε)methyl groups, which results in the formation of unstable hemiaminal intermediates that spontaneously decompose to yield formaldehyde and the residual di- or monomethylated lysine residue; in vivo, however, the enzyme only demethylates trimethylated residues.[17a,18] Accordingly, the binding of 2-oxoglutarate (**1**) is crucial for the molecular interaction. Compounds that mimic this acid might interfere with the catalytic mechanism.[19] Recently, it could be shown that the well-known and widely used

[a] *N. Rüger, Dr. T. Emmrich, Prof. Dr. A. Link*
Institute of Pharmacy, Ernst-Moritz-Arndt-Universität Greifswald
Friedrich-Ludwig-Jahn-Str. 17, 17487 Greifswald (Germany)
E-mail: Link@uni-greifswald.de

[b] *M. Roatsch, Prof. Dr. M. Jung*
Institute of Pharmaceutical Sciences, Albert-Ludwigs-Universität Freiburg
Albertstr. 25, 79104 Freiburg (Germany)

[c] *Dr. H. Franz, Prof. Dr. R. Schüle*
University of Freiburg Medical Center
Department of Urology, Women's Hospital and Center for Clinical Research
Breisacher Str. 66, 79106 Freiburg (Germany)

Supporting information for this article is available on the WWW under http://dx.doi.org/10.1002/cmdc.201500335.

plant growth regulator daminozide (**2**, succinic acid 2,2-dimethylhydrazide) selectively inhibits KDM2A but neither KDM3A, KDM4E, KDM5C, KDM6B nor PHD2 (hypoxia-inducible factor prolyl hydroxylase), predominantly by competitive inhibition with respect to **1** ($K_i = 1.97$ μM).[20] In contrast, other known inhibitors such as 8-hydroxyquinoline-5-carboxylic acid (IOX1, **3**) are pan-KDM inhibitors that inhibit KDM2A, KDM3A, KDM4E, KDM5C, and KDM6B to a similar extent (Figure 1).[21] One of the

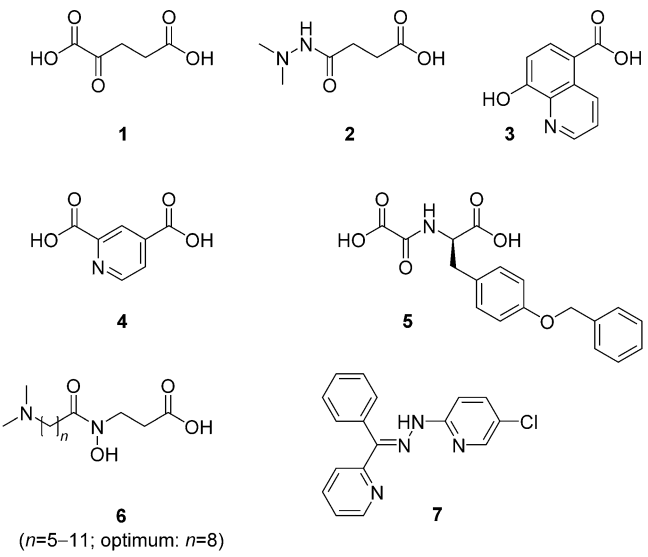

Figure 1. Endogenous substrate 2-oxoglutarate (**1**) and a selection of published inhibitors of JumonjiC-domain-containing histone demethylases **2**–**7**.

earlier discovered KDM inhibitors with remarkable potency but low selectivity is pyridine-2,4-dicarboxylic acid (**4**),[22] which frequently serves as a standard against which other inhibitors are compared in vitro. Due to their ionic character, none of the aforementioned ligands is able to penetrate intact cell membranes, which renders them unfeasible for any cell-based studies. This drawback was overcome for the first time by Hamada et al. with their design of 2-oxoglutarate mimics that contain a long alkyl chain (compound **6**).[23] A structurally unique approach in this field was recently published by Wang et al.[24] The *E* isomer of JIB-04 (**7**) is a strong, cell-active KDM4 inhibitor with highest selectivity for KDM4D (JMJD2D); however, it is not competitive against **1**. An up-to-date review regarding known demethylase inhibitors is provided by Thinnes et al.[25]

The pioneering work of the group of Schofield et al. has led to a deeper understanding of the binding mode of experimental inhibitors of KDM4A.[2] Compounds with a core structure closely resembling that of **1**, such as *O*-benzyl-*N*-(carboxycarbonyl)-D-tyrosine (**5**),[26] which is essentially a derivative of the known JmjC inhibitor *N*-oxalylglycine,[13] bind in a way that the carboxylate group of the tyrosine moiety forms hydrogen bonds and ionic interactions with protonated Lys206 and the phenolic hydroxy group of Tyr132. The second carboxyl group acts as a hydrogen bond donor toward Ser288 and a hydrogen bond acceptor toward Ser196. Together with the adjacent amide group, this α-keto acid mimic complexes a divalent cation (here Ni^{2+} instead of Fe^{2+} for stability reasons) that is held in place by His188, His276, and Glu190 (Figure 2).

The conformationally unconstrained **5** inhibits KDM4A with an IC_{50} value of 33 μM. Although the crystal structure of **5** with

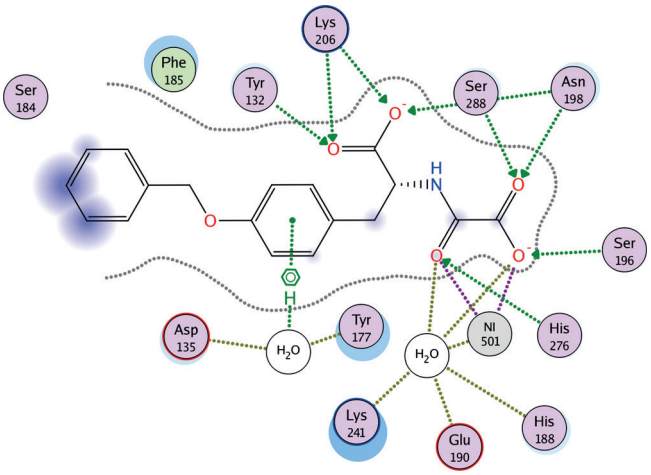

Figure 2. Interactions of *O*-benzyl-*N*-(carboxycarbonyl)-D-tyrosine (**5**) and KDM4A (image based on PDB 2WWJ).[26]

KDM4A indicates occupation of a large hydrophobic pocket adjacent to the substrate binding cleft, the contribution of the lipophilic interactions or π–π stacking of the phenyl and benzyl moieties to Phe185 and Lys241 is only weakly pronounced.[26] Considering this information, we designed a series of acidic fragment-like molecules as potential inhibitors of 2-oxoglutarate-dependent demethylases. Among the considerable arsenal of iron chelating warheads such as hydroxamic acids or diphenols, there is also the acylhydrazide function. Thus, we decided to start with this motif as a replacement for the α-keto acid moiety due to the success of this functional group present in the proof-of-principle selective inhibitor **2**. The known binding mode of this inhibitor served as a starting point for the selection of our iron binding warhead. In contrast to the dimethyl substitution of **2**, unsubstituted hydrazides were prepared with a focus on ease of generation of analogues by condensation with carbonyl compounds as, still metal complexing, hydrazones.

At the same time, we reasoned that it would be beneficial to replace the second carboxylic acid of 2-oxoglutarate by a tetrazole moiety which was unprecedented in this area. However, the bioisosteric replacement of carboxylic acids by tetrazoles has led to active compounds including many drugs in the market, for example, diuretics and AT_1 receptor antagonists. Size, pK_a and electrostatic potential of carboxyl and tetrazolyl groups are similar, whereas tetrazoles are more lipophilic, thus facilitating membrane penetration.[27] Based on these findings, it should be possible to identify fragment-like inhibitors that complex the divalent cation and form hydrogen bonds and ionic interactions with protonated Lys206 and the phenolic hydroxy group of Tyr132 in a favorable manner.

Results and Discussion

The optimal distance between the two interaction motifs, that is, metal chelating moiety and anionic center, was uncertain. Based on visual inspection of available crystal structures (e.g., PDB 4AI9[20]) we envisioned the synthesis of three homologous hydrazides by established procedures in a three-step reaction and subjecting them to biological evaluation (see Scheme 1, Table 1).

First, the chlorinated acid esters **8b–c** were converted into the corresponding nitriles **9b–c** in good yields (79–83%),[28] followed by ammonium chloride catalyzed cyclization with sodium azide in DMF to obtain the corresponding 5-tetrazoles **10a–c**.[29] Yields ranged between 15–56% and decreased with increasing chain length between the tetrazole ring and the carbonyl group, because of the diminished activation of the nitrile moiety. Subsequently, intermediates **10a–c** were subjected to hydrazinolysis in quantitative yields.

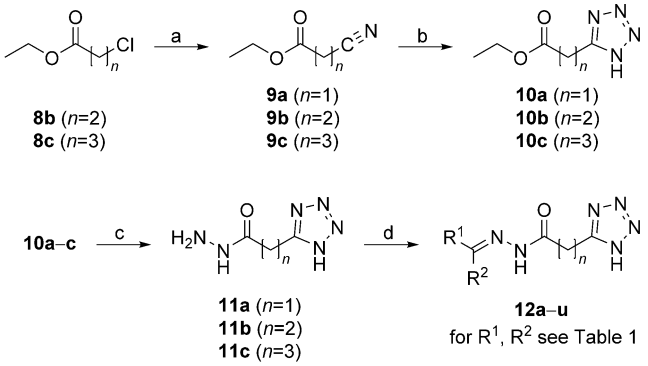

Scheme 1. Synthesis of tetrazolylhydrazides **11a–c** with varying spacer length. *Reagents and conditions*: a) NaCN, DMSO, 3 h, 50 °C→15 h, RT; b) NaN_3, NH_4Cl, DMF, 8–24 h, 95–125 °C; c) H_2N-NH_2, microwave, 5 min, 115 °C; d) appropriate carbonyl component, MeOH, microwave, 2 min, 80 °C.

Table 1. Residues R^1 and R^2 in **12a–u**.

Compd[a]	R^1	R^2
12a	CH_3	4-pyridyl
12b	CH_3	4-methoxyphenyl
12c	H	phenyl
12d	CH_3	phenyl
12e	H	4-methoxyphenyl
12f	CH_3	CH_3
12g	CH_3CH_2	CH_3CH_2
12h		$-(CH_2)_4-$
12i	H	4-(dimethylamino)phenyl
12j	H	4-(trifluoromethyl)phenyl
12k	H	4-chlorophenyl
12l	H	4-cyanophenyl
12m	H	4-bromophenyl
12n	CH_3	4-methylphenyl
12o	H	4-nitrophenyl
12p	CH_3	4-nitrophenyl
12q	H	4-methylphenyl
12r	H	2-methylphenyl
12s	H	cinnamyl
12t	H	4-ethylphenyl
12u	H	2-methoxyphenyl

[a] See Supporting Information S5 for compound characterization.

Counterintuitively, the tetrazolyl acylhydrazide with the smallest distance of the interaction motifs, **11a**, was the most active compound with an IC_{50} value of 46.64 ± 0.94 μM in a formaldehyde dehydrogenase (FDH)-coupled assay (see Table 2; enzyme concentration c_{enz} = 2.4 μM). In the antibody-based LANCE assay that employs far less enzyme (c_{enz} = 60 nM), the potency is as high as 2.38 ± 0.37 μM. Pyridine-2,4-dicarboxylic acid (**4**) was used as positive control in both assays. Similar differences have also been observed for the reference inhibitor JIB-04 (**7**), which includes a hydrazone moiety, with 17.6 μM in the FDH assay and 4.1 μM in the LANCE assay.[24] As **7** showed cellular activity even at 1 μM, at least in this case the FDH assay rather seems to underestimate potency which is encouraging for our results. By employing the LANCE assay, we were able to exclude FDH inhibition as a confounder. Either way, with respect to the relative molar mass (M_r = 142 Da) of this fragment-like inhibitor, this activity is remarkable. To evaluate the importance of the acidic tetrazole ring for inhibitory activity, a series of related acetohydrazides with substituted and unsubstituted aromatic or heteroaromatic rings (Figure 3), as well as the ring-methylated derivative **20** of lead **11a** were prepared (see Scheme 3 below). Derivative **20** lacks the acidic properties of an unsubstituted 5-tetrazole, while still exhibiting chelating properties.

Table 2. In vitro activity of derivatives against isolated KDM4A in the FDH and LANCE assays.

Compd[a]	IC_{50} [μM]	
	FDH	LANCE
4 (control)	1.37 ± 0.39	0.0337 ± 0.007
11a	46.64 ± 0.94	2.38 ± 0.37
11b	64.1 ± 12.8	8.32 ± 1.08
11c	69.8 ± 15.5	7.68 ± 1.54
12f	391 ± 61	11.80 ± 0.38
12g	154 ± 42	6.2 ± 1.5

[a] All other compounds of the series **11** and **12** were tested as well, but were devoid of activity (see Supporting Information S5).

While the tetrazole ring could be built up via cycloaddition reaction, hydrazides **11d–l** were prepared by different routes (Scheme 2). Pyridylacetohydrazides **11d–f** were synthesized by chlorinating the corresponding pyridylmethanols **13a–c**, followed by Kolbe nitrile synthesis of the chloromethylpyridyl hydrochlorides **14a–c**[30] and saponification of the resulting nitriles **15a–c** in the presence of a short-chained alcohol to obtain esters **10d–f**, directly.[31] These esters were subsequently subjected to hydrazinolysis. Pyrazole and imidazole acetohydrazides **11g** and **11h** were obtained by alkylating the heterocycles with ethyl bromoacetate (**16**), followed by hydrazinolysis of intermediates **10g** and **10h**.

Hydrazide **11i** was prepared from the commercially available ethyl ester precursor, and compounds **11j–l** could be obtained directly from the corresponding carboxylic acids, following

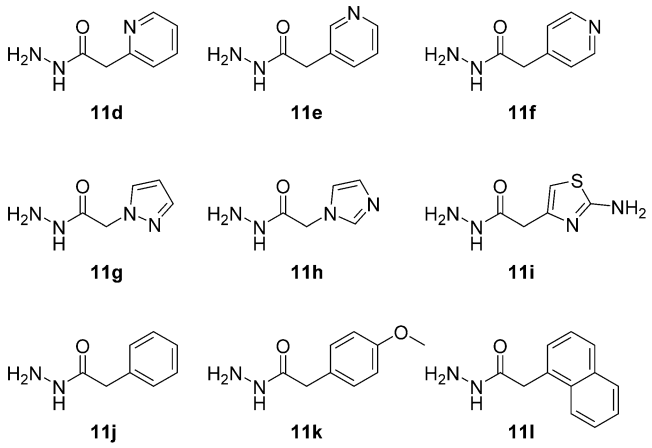

Figure 3. Inactive hydrazides **11 d–l** devoid of an acidic heterocyclic ring.

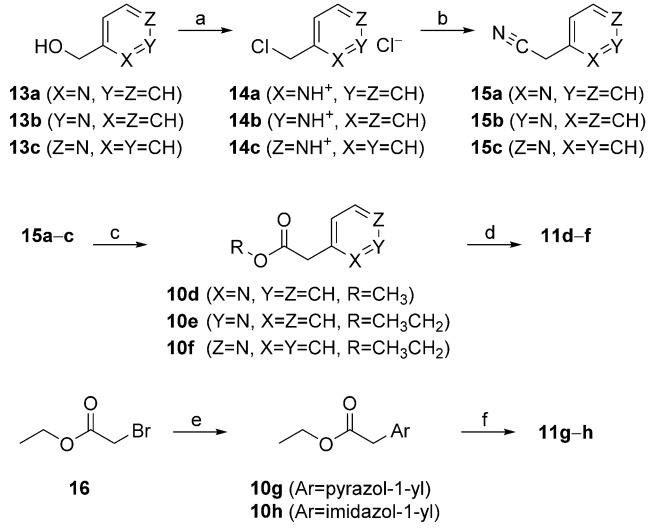

Scheme 2. Synthesis of hydrazides **11 d–h**. *Reagents and conditions*: a) $SOCl_2$, 3 h, 60 °C; b) NaCN, DMSO, 2.5 h, 30–40 °C; c) HCl, ROH, 21 h, reflux; d) H_2N-NH_2, 8 h, 80 °C; e) Cs_2CO_3, DMF, 1–24 h, RT; f) H_2N-NH_2, 1–16 h, 80 °C.

a procedure described by Rabini and Vita.[32] All these variations proved to be inactive (Figure 3), underlining the importance of the tetrazole moiety for efficient binding.

For the synthesis of ring-methylated tetrazolylhydrazide **20**, diethyl 2-(ethoxymethylene)malonate (**17**) was transformed into isoxazolone **18**, which could be easily converted in the course of a ring-opening-recyclization tandem reaction into ethyl tetrazolylacetate **19**.[33] As before, this ester was subjected to hydrazinolysis, thus yielding the desired nonacidic tetrazole **20** (Scheme 3), which expectedly did not show any notable activity against KDM4A at concentrations up to 200 and 400 μM in the LANCE and FDH assays, respectively.

As further proof of principle, we tested the ester **10 a** lacking the hydrazide function, and could show that this interaction motif is essential for enzyme inhibition by the expected negative outcome. The in vitro data for all compounds tested as inactive are summarized in the Supporting Information (see Supporting Information S5).

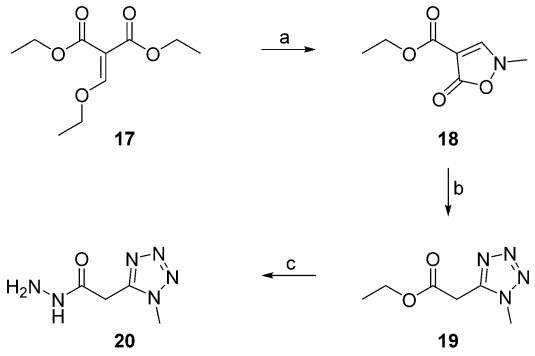

Scheme 3. Synthesis of tetrazolylhydrazide **20**. *Reagents and conditions*: a) CH_3NHOH, Na_2CO_3, 16 h, RT; b) NaN_3, H_2O, 7 h, RT; c) H_2N-NH_2, EtOH, 8 h, 60 °C.

Because both tetrazole derivatives and acyl hydrazides are widely recognized as versatile metal chelators, we considered it necessary to determine the inhibition mechanism of **11 a**, in order to exclude ejection of enzyme-bound metal ions as the modus operandi. In fact, zinc-ejecting KDM4A inhibitors have been reported, for example, ebselen and disulfiram,[34] and such a behavior was not unexpected for **11 a**. However, inhibition experiments in the presence of various concentrations of **1** clearly revealed **11 a** to be a competitive inhibitor with regard to the endogenous substrate (see Figure 4). The K_i value was 1.974 μM, which again demonstrates that values obtained with the FDH assay seem to underestimate compound potency. The iron chelators EDTA and deferoxamine were used as controls, and gave markedly different results (see Supporting Information S4).

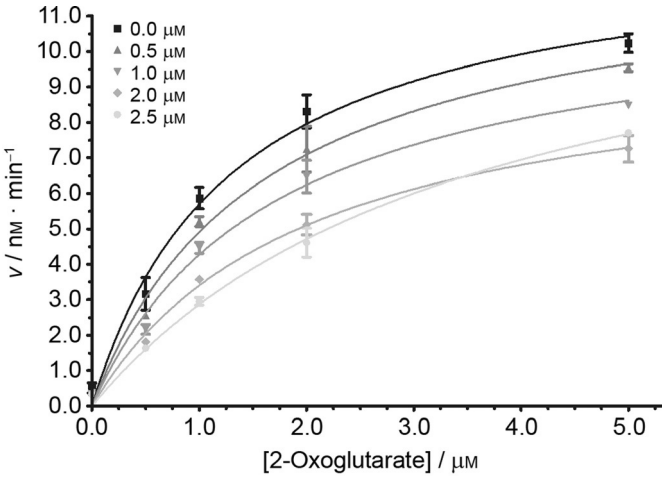

Figure 4. Determination of the inhibition kinetics of **11 a** against KDM4A in the LANCE assay. Various concentrations were assayed against the endogenous substrate, 2-oxoglutarate (**1**), in a competition assay. The results show that ejection of protein-bound metal can be excluded as the inhibiting mechanism; **11 a** rather inhibits KDM4A competitively.

We were furthermore surprised to find that **11a** displayed a relative selectivity of ~4- and 41-fold for KDM4A relative to KDM5A (JARID1A) and KDM6B (JMJD3), respectively, in the LANCE assay (Table 3). This is quite remarkable, considering the simple structure and the fragment-like character of this compound. As control, we employed again **4**, which has been described as a rather unselective, broad-spectrum KDM inhibitor,[35] a finding that we were able to confirm. To also include a control with relative selectivity, we used the bipyridyl derivative GSK-J1, which was recently discovered in a high-throughput screening by researchers at GlaxoSmithKline.[36] The compound was initially described as being highly selective for demethylases KDM6A and KDM6B, although Heinemann et al. shortly after demonstrated that this statement did not represent the whole picture. In fact, several KDM5 isoenzymes, in particular KDM5B, were only five- to tenfold less affected.[37] Nonetheless is GSK-J1 still one of the most potent and (relatively) selective KDM inhibitors known to date and was therefore considered a suitable control. In comparison with GSK-J1, our acylhydrazide **11a** showed a unique selectivity profile, which cannot be found with any other known KDM inhibitor. We also tested **11a** against histone deacetylase 1 (HDAC1) in a standard trypsin-based assay,[38] where it did not show any notable activity (data not shown).

Table 3. Selectivity screening of **11a** and two selected reference inhibitors: activity against isolated KDM4A, KDM5A, and KDM6B in the FDH and LANCE assays.

Compd	IC_{50} [μM]			
	KDM4A (JMJD2A)		KDM5A (JARID1A)	KDM6B (JMJD3)
	FDH[b]	LANCE[c]	LANCE[d]	LANCE[e]
11a	46.6 ± 0.9	2.38 ± 0.37	10.41 ± 1.80	98.0 ± 7.2
4	0.70 ± 0.03	0.034 ± 0.007	0.1000 ± 0.028	36.0 ± 4.7
GSK-J1[a]	NI[f]	54.4 ± 1.6	0.418 ± 0.153	0.128 ± 0.018

[a] 3-{[2-(Pyridin-2-yl)-6-(1,2,4,5-tetrahydro-3*H*-benzo[*d*]azepin-3-yl)pyrimidin-4-yl]amino}propanoic acid.[32] [b] Enzyme 1.75 μM, peptide 35 μM, 60 min, 37 °C. [c] Enzyme 60 nM, peptide 400 nM, 45 min, RT. [d] Enzyme 25 nM, peptide 100 nM, 45 min, RT. [e] Enzyme 50 nM, peptide 400 nM, 120 min, RT. [f] No inhibition at 400 μM.

The combined results encouraged us to select tetrazolyl acetohydrazide **11a** as a lead structure for the synthesis of derivatives, because its small size results in high ligand efficiencies of 0.59 (FDH assay) and 0.78 (LANCE assay),[39] which is a very good starting point for further studies. To generate arrays of derivatives of **11a**, we prepared hydrazones **12a–u** with various carbonyl compounds aiming to increase the binding affinity. Disappointingly, none of these derivatives showed improved activity, and the majority of the synthesized compounds were actually devoid of any activity (Table 2). Seemingly, all prepared hydrazones were sterically too demanding. Further work regarding the derivatization of our newly found lead is under way and will be reported soon.

Conclusions

To identify a novel starting point for inhibitors of histone lysine demethylase 4A, we developed a fragment-like compound, 5-tetrazolyl acetohydrazide (**11a**). The half-maximal inhibitory concentrations were found to be 46.64 ± 0.94 and 2.38 ± 0.37 μM in enzyme-coupled and antibody-based assays, respectively. It is competitive with regard to the co-substrate 2-oxoglutarate (**1**) with a K_i value of ~2 μM. Based on the mechanism of inhibition and its structural features, we propose a binding mode similar to those of well-known KDM4A inhibitors, that is, via complexation of the active center Fe^{II} ion with the acyl hydrazide moiety, and formation of a salt bridge with Lys206 and a hydrogen bond with Tyr132 through the acidic tetrazole ring (Figure 5). The latter is thus far unprecedented.

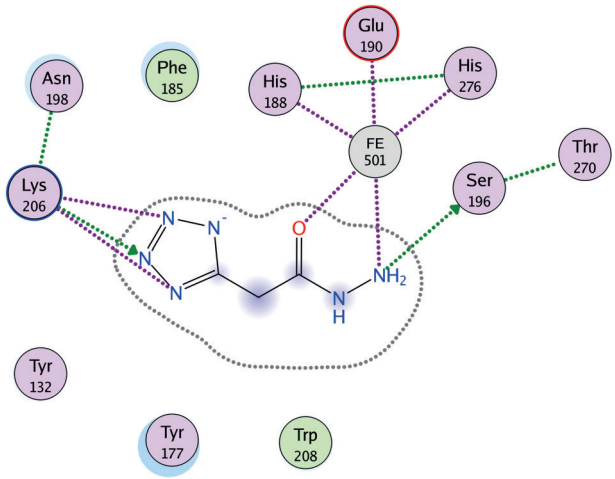

Figure 5. Proposed binding mode of lead fragment **11a**. The depicted interactions were anticipated in analogy to published resolved crystal structures with co-crystallized inhibitors.[13,15,16,17b,20,21,26,40] Further support comes from the results of the in vitro testing of our compounds that either lack the acylhydrazide motif (**10a**), the tetrazole ring (**11d–l**), or where the tetrazole ring was methylated, thus abolishing its acidic nature (**20**).

As Schofield et al. previously demonstrated by using substrate analogous peptide fragments, linking of ligands of the 2-oxoglutarate and substrate binding sites enables potent and highly selective inhibition of JmjC histone demethylases.[16] Thus, we suggest use of the novel lead presented herein as an anchor point to target the 2-oxoglutarate binding site and to grow this fragment into a selective and tight-binding inhibitor of Jumonji-domain-containing histone demethylases with drug-like properties.

The central question, whether metal complexing drugs are more promiscuous than other drugs due to nonspecific metal chelation, is still under debate. Experimental results from Day and Cohen should help to spark renewed interest in such compounds.[41] They screened marketed and experimental metalloenzyme-inhibiting drugs against a panel of metalloproteins such as HDAC and ACE. Even at high inhibitor concentrations (10 μM), off-target inhibition was limited. As expected, off-target inhibition was most pronounced among metalloen-

zymes incorporating the same catalytic metal, active site structure, and functionality, and was more common among early-stage lead compounds than in fully developed inhibitors. Almost all approved drugs showed no off-target inhibition, regardless of the complexing warhead, suggesting that inhibitor selectivity is a combination of metal binding and the supportive backbone interactions. Therefore, metal chelating inhibitors of metalloproteins should no longer be automatically associated with high risk for indiscriminate off-target inhibition of metalloenzymes, and their development poses no more risk for nonspecific activity than small-molecule inhibitors of metal-independent enzymes. After all, the relative selectivity of our fragment-like lead **11a** for KDM4A, and the lack of activity against HDAC1 seem to support these findings.

Experimental Section

General. All starting materials (aldehydes and ketones, halogenated acid esters, aromatic heterocycles) and solvents, unless otherwise noted, were obtained from Sigma Aldrich or ABCR GmbH & Co. KG and used without further purification. Medium pressure liquid chromatography (MPLC) was done on silica gel from Macherey–Nagel (particle size 50–100 μm, 140–270 mesh ASTM) with Büchi devices C-630, C-601 and C-660 (column length 40 cm, column diameter 3.5 cm). Melting points were determined on a hot stage microscope by Kofler PHMK 81/3035 "Boëtius" (VEB Wägetechnik Rapido) with 16-fold amplification or Büchi melting point apparatus M-565 and are uncorrected. Microwave-assisted synthesis was performed using a Discover LabMate ('closed vessel' mode, 10 mL total capacity vessel, temperature control via IR sensor) from CEM. The parameter 'PowerMax' indicates a permanent radiation of microwaves simultaneously to intense cooling. The specified purities were determined by the 100% method of the DAD chromatogram at wavelengths as indicated. Acylhydrazones are subject to isomerism at the amide moiety; when both isomers could be resolved chromatographically, purity values apply for both isomers together. NMR spectra were recorded using an Avance III instrument with Ultrashield 400 (^{1}H: 400.2 MHz, ^{13}C: 100.6 MHz) from Bruker at 25 °C with tetramethylsilane (TMS) as internal standard, using the ppm scale. High-resolution mass spectra (HRMS) were obtained after high-performance liquid chromatography (HPLC) with a mass spectrometer (LC-IT-TOF) from Shimadzu based on a deviance tolerance limit $\leq$5 ppm. Mid-infrared spectra were recorded on a Nicolet IR200 FT-IR from Thermo Electron Corporation with diamond ATR accessory. Figures 2 and 5 were prepared using LigPlot.[42]

General procedure for the synthesis of compounds 9a–c: NaCN (1.5 equiv) was suspended in DMSO at room temperature. Subsequently, the appropriate chlorinated acid ester (1.0 equiv) was added dropwise while the temperature of the resulting mixture was kept at 40 °C. The suspension was then heated at 50 °C for 3 h and stirred for another 15 h at room temperature. NaOH was added and the reaction mixture was diluted with H_2O until all solids had dissolved. The solution was exhaustively extracted with Et_2O, dried over Na_2SO_4 and concentrated under reduced pressure to obtain a colorless oil.

Ethyl 2-cyanoacetate (9a): This compound was commercially available.

Ethyl 3-cyanopropanoate (9b): With halogenated ester **8b** (20.0 g, 150 mmol), NaCN (10.5 g, 220 mmol), DMSO (45 mL) and NaOH (1.50 g), compound **9b** was obtained as a colorless oil (15.1 g, 119 mmol, 79%); purity: 92% (at 220 nm); ^{1}H NMR ([D$_6$]DMSO): δ = 1.20 (t, J = 7.1 Hz, 3H), 2.68 (s, 4H), 4.11 ppm (q, J = 7.1 Hz, 2H); ^{13}C NMR ([D$_6$]DMSO): δ = 12.4, 14.0, 29.2, 60.5, 119.8, 170.6 ppm; IR (ATR): $\tilde{\nu}$ = 2250 (w), 1729 cm^{-1} (s); HRMS (ESI) m/z [M+H$^+$] calcd for $C_6H_{10}NO_2^+$: 128.0712, found: 128.0701.

Ethyl 4-cyanobutanoate (9c): With halogenated ester **8c** (50.0 g, 332 mmol), NaCN (23.9 g, 498 mmol), DMSO (113 mL) and NaOH (3.00 g), compound **9c** was obtained as a colorless oil (38.9 g, 276 mmol, 83%); purity: 100% (at 220 nm); ^{1}H NMR ([D$_6$]DMSO): δ = 1.19 (t, J = 7.1 Hz, 3H), 1.81 (qu, J = 7.3 Hz, 2H), 2.40 (t, J = 7.3 Hz, 2H), 2.53 (t, J = 7.3 Hz, 2H), 4.07 ppm (q, J = 7.1 Hz, 2H); ^{13}C NMR ([D$_6$]DMSO): δ = 14.0, 15.6, 20.5, 32.2, 60.0, 120.2, 171.8 ppm; IR (ATR): $\tilde{\nu}$ = 2245 (w), 1727 cm^{-1} (s); HRMS (ESI) m/z [M+H$^+$] calcd for $C_7H_{11}NO_2^+$: 142.0868, found: 142.0869.

General procedure for the synthesis of compounds 10a–c: The appropriate cyano acid ester (1.0 equiv), NaN_3 (1.1 equiv) and NH_4Cl (0.2 equiv) were suspended in DMF. The reaction mixture was heated at 95–125 °C for 8–24 h. Subsequently the solvent was removed under reduced pressure. The resulting residue was diluted with H_2O and adjusted to pH 1 with concentrated hydrochloric acid (CAUTION: Release of HN_3!). The desired product was obtained by precipitation or extraction.

Ethyl 2-(1*H*-tetrazol-5-yl)acetate (10a): With cyano acid ester **9a** (23.0 g, 200 mmol), NaN_3 (14.3 g, 220 mmol), NH_4Cl (2.30 g, 43 mmol), DMF (220 mL) and H_2O (220 mL) for 8 h at 95 °C. The reaction was worked up by filtering off the precipitate, followed by recrystallization from propan-2-ol, to obtain compound **10a** as a colorless solid (17.6 g, 113 mmol, 56%); purity: 70% (at 220 nm); mp: 125 °C; ^{1}H NMR ([D$_6$]DMSO): δ = 1.21 (t, J = 7.0 Hz, 3H), 4.12–4.17 (q, J = 7.0 Hz, 2H), 4.17 (s, 2H), 16.34 ppm (s, 1H); ^{13}C NMR ([D$_6$]DMSO): δ = 14.0, 29.5, 61.3, 150.4, 167.7 ppm; IR (ATR): $\tilde{\nu}$ = 1741 cm^{-1} (s); HRMS (ESI) m/z [M+H$^+$] calcd for $C_5H_9N_4O_2^+$: 157.0726, found: 157.0727.

Ethyl 3-(1*H*-tetrazol-5-yl)propanoate (10b): With cyano acid ester **9b** (17.8 g, 140 mmol), NaN_3 (10.0 g, 154 mmol), NH_4Cl (1.80 g, 34 mmol), DMF (70 mL) and H_2O (70 mL) for 8 h at 105 °C. The crude solution was worked up by diluting with brine and extracting exhaustively with EtOAc, drying the combined organic phases over Na_2SO_4 and concentrating under reduced pressure. The resulting colorless oil was cooled to −18 °C, filtering off the resulting precipitate and washing with Et_2O gave compound **10b** as a colorless solid (9.47 g, 55.7 mmol, 42%); mp: 84–85 °C; ^{1}H NMR ([D$_6$]DMSO): δ = 1.16 (t, J = 7.0 Hz, 3H), 2.83 (t, J = 7.2 Hz, 2H), 3.12 (t, J = 7.2 Hz, 2H), 4.06 (q, J = 7.0 Hz, 2H), 16.04 ppm (s, 1H); ^{13}C NMR ([D$_6$]DMSO): δ = 14.0, 18.5, 30.7, 60.2, 155.2, 171.4 ppm; IR (ATR): $\tilde{\nu}$ = 1719 cm^{-1} (s); HRMS (ESI) m/z [M+H$^+$] calcd for $C_6H_{11}N_4O_2^+$: 171.0882, found: 171.0878.

Ethyl 4-(1*H*-tetrazol-5-yl)butanoate (10c): With cyano acid ester **9c** (38.0 g, 270 mmol), NaN_3 (19.3 g, 297 mmol), NH_4Cl (3.80 g, 72 mmol), DMF (135 mL) and H_2O (135 mL) for 24 h at 125 °C. To work up the solution, it was exhaustively extracted with EtOAc, the collected organic phases dried over Na_2SO_4 and concentrated under reduced pressure. The orange oil was cooled to −18 °C, filtering off the resulting precipitate and recrystallization from Et_2O gave compound **10c** as a colorless solid (7.50 g, 40.8 mmol, 15%); mp: 49–52 °C; ^{1}H NMR ([D$_6$]DMSO): δ = 1.18 (t, J = 7.1 Hz, 3H), 1.96 (qu, J = 7.4 Hz, 2H), 2.39 (t, J = 7.4 Hz, 2H), 2.92 (t, J = 7.4 Hz, 2H), 4.06 (q, J = 7.1 Hz, 2H), 16.04 ppm (s, 1H); ^{13}C NMR ([D$_6$]DMSO): δ = 14.0, 21.9, 22.2, 32.4, 59.8, 155.4, 172.2 ppm; IR (ATR): $\tilde{\nu}$ =

1723 cm^{-1} (s); HRMS (ESI) *m/z* $[M+H^+]$ calcd for $C_7H_{13}N_4O_2^+$: 185.1039, found: 185.1030.

General procedure for the synthesis of compounds 11 a–c: The appropriate tetrazole acid ester (1.0 equiv) and hydrazine hydrate (80% ≙ 50% hydrazine, 3.0–12.3 equiv) were heated by microwave irradiation (p_{max} = 17 bar, T_{max} = 115 °C, P_{max} = 200 W, ramp time = 1 min, hold time = 5 min, continuous irradiation and stirring).

2-(1*H*-Tetrazol-5-yl)acetohydrazide (11 a): With tetrazole acid ester **10 a** (16.6 g, 106 mmol) and hydrazine hydrate (20.6 g, 318 mmol). EtOH (50 mL) was added and the solution cooled to 0 °C. Filtering off the resulting precipitate and washing with EtOH gave compound **11 a** as a colorless solid (16.3 g, 110 mmol, > 95%); purity: 100% (at 220 nm); mp: 158–159 °C; ^{1}H NMR ([D$_6$]DMSO): δ = 3.52 ppm (s, 2H); ^{13}C NMR ([D$_6$]DMSO): δ = 31.6, 155.5, 168.5 ppm; IR (ATR): $\tilde{\nu}$ = 1675 (m), 1624 (w), 1568 (w), 1525 cm^{-1} (w); HRMS (ESI) *m/z* $[M+H^+]$ calcd for $C_3H_7N_6O^+$: 143.0681, found: 143.0669.

3-(1*H*-Tetrazol-5-yl)propanehydrazide (11 b): With tetrazole acid ester **10 b** (7.91 g, 46 mmol) and hydrazine hydrate (30.9 g, 469 mmol). EtOH (20 mL) was added and the solution cooled to −18 °C. Filtering off the resulting precipitate and washing with EtOH gave compound **11 b** as a colorless solid (7.38 g, 47 mmol, > 95%); purity: 100% (at 220 nm); mp: 136–139 °C; ^{1}H NMR ([D$_6$]DMSO): δ = 2.38–2.42 (m, 2H), 2.85–2.90 ppm (m, 2H); ^{13}C NMR ([D$_6$]DMSO): δ = 21.4, 33.1, 159.6, 171.3 ppm; IR (ATR): $\tilde{\nu}$ = 1596 (m), 1567 cm^{-1} (m); HRMS (ESI) *m/z* $[M+H^+]$ calcd for $C_4H_9N_6O^+$: 157.0838, found 157.0835.

4-(1*H*-Tetrazol-5-yl)butanehydrazide (11 c): With tetrazole acid ester **10 c** (7.06 g, 38 mmol) and hydrazine hydrate (30.9 g, 469 mmol). All volatiles were removed under reduced pressure and residual hydrazine removed by azeotropic distillation with EtOH. Recrystallization from MeOH/Et$_2$O 3:1 gave compound **11 c** as a colorless solid (6.04 g, 36 mmol, 93%); purity: 100% (at 220 nm); mp: 113–115 °C; ^{1}H NMR ([D$_6$]DMSO): δ = 1.82 (qu, *J* = 7.6 Hz, 2H), 2.06 (t, *J* = 7.6 Hz, 2H), 2.66 ppm (t, *J* = 7.6 Hz, 2H); ^{13}C NMR ([D$_6$]DMSO): δ = 24.4, 24.8, 33.1, 159.6, 171.5 ppm; IR (ATR): $\tilde{\nu}$ = 3288 (m), 1648 (s), 1521 cm^{-1} (m); HRMS (ESI) *m/z* $[M+H^+]$ calcd for $C_5H_{11}N_6O^+$: 171.0994, found: 171.0990.

Purification of KDM4A. The plasmid pNIC28-Bsa4 JMJD2A encoding human KDM4A residues 1–359 was used for expression and purification as described by Ng et al. with minor modifications.[13] Shortly, the expression construct was transformed in BL21-CodonPlus-Ril competent cells. Six liters of TB media containing kanamycin (50 μg mL^{-1}) and chloramphenicol (34 μg mL^{-1}) were inoculated with a 15 mL L^{-1} overnight culture and grown at 37 °C. Expression was induced by addition of 0.2 mM IPTG at A_{260} = 0.6. Then the culture was incubated at 18 °C for another 18 h. After harvesting and lysis of the bacteria, the protein was purified by Talon bead column. The purity of KDM4A estimated by SDS-PAGE was > 90%.

KDM4A FDH assay. The formaldehyde dehydrogenase (FDH) enzyme-coupled demethylase activity assay was performed in a total volume of 20 μL on white OptiPlate-384 microtiter plates (PerkinElmer, Waltham, MA, USA) using a 50 mM HEPES buffer at pH 7.50 containing 0.01% Tween-20. A solution of 0.10 mg mL^{-1} (2.4 μM) KDM4A 1–359 was pre-incubated with compound solutions of varying concentration (0–400 μM) in DMSO at room temperature for 10 min. A substrate solution containing 100 μM ascorbic acid, 10 μM $FeSO_4$, 0.001 U·μL^{-1} FDH, 500 μM NAD^+, 50 μM 2-oxoglutarate, and 35 μM of H3K9me$_3$ substrate peptide ARK(me$_3$)-STGGK-NH_2 (Peptide Specialty Laboratories, Heidelberg, Germany) was added (final concentrations). Final DMSO concentration was 2% in all wells. Fluorescence intensity of the forming product NADH was measured at λ_{ex} = 330 nm and λ_{em} = 460 nm on a POLARstar Optima microplate reader (BMG Labtech, Ortenberg, Germany) immediately after addition (t = 0) and after one hour of incubation on a horizontal shaker at 37 °C. Values were blank-corrected and the difference in intensity at t = 1 h and t = 0 was taken as a measurement of enzyme activity. Activity in percent is in comparison with compound-free DMSO control and no-substrate negative control. Inhibition curves were analyzed by sigmoidal curve fitting using GraphPad Prism 4.00 and IC_{50} values calculated from the fit parameters as mean ± SD from two independent experiments.

KDM4A LANCE assay. The commercial antibody-based LANCE*Ultra* demethylase activity assay (PerkinElmer, Waltham, MA, USA) was performed in a total volume of 10 μL on white OptiPlate-384 microtiter plates (PerkinElmer) using a 50 mM HEPES buffer at pH 7.50 containing 0.01% Tween-20 and 0.01% BSA. A solution of 60 nM KDM4A 1–359 was pre-incubated with compound solutions of varying concentration (0–1000 μM) in DMSO at room temperature for 10 min. A substrate solution containing 100 μM ascorbic acid, 5 μM $FeSO_4$, 1 μM 2-oxoglutarate, and 400 nM of biotinylated H3K9me$_3$ substrate peptide ARTKQTARK(me$_3$)-STGGKAPRKQLA-GGK(biotin) (BPS Bioscience, San Diego, CA, USA) was added (final concentrations). Final DMSO concentration was 5% in all wells. Plates were incubated on a horizontal shaker at room temperature for 45 min. Reactions were stopped by addition of 10 μL of detection mix containing 2 nM europium-labeled anti-H3K9me$_2$ LANCE antibody (PerkinElmer), 50 nM U*Light*-streptavidin dye (PerkinElmer), and 1 mM EDTA in 1× LANCE detection buffer (PerkinElmer) (final concentrations). Plates were again incubated on a horizontal shaker at room temperature for 60 min. FRET intensity was measured on an EnVision 2102 multilabel plate reader (PerkinElmer) at λ_{ex} = 340 nm and λ_{em} = 665 nm with a delay of 100 μs. Values were blank-corrected and activity in percent is in comparison with compound-free DMSO control and no-enzyme negative control. Inhibition curves were analyzed by sigmoidal curve fitting using GraphPad Prism 4.00 and IC_{50} values calculated from the fit parameters as mean ± SD from two independent experiments.

KDM5A LANCE assay. The antibody-based LANCE*Ultra* activity assay for KDM5A (JARID1A) was performed essentially as described for JMJD2A (KDM4A) with the following modifications: A solution of 25 nM full-length JARID1A 1–1090 (BPS BioScience, San Diego, CA, USA) was used with 100 nM biotinylated H3K4me$_3$ 1–21 substrate peptide ARTK(me$_3$)-QTARKSTGGKAPRKQLA-GGK(biotin) (AnaSpec, Fremont, CA, USA). The detection mix contained the appropriate europium-labeled anti-H3K4me$_2$/me$_1$ LANCE antibody (PerkinElmer).

KDM6B LANCE assay. The antibody-based LANCE*Ultra* activity assay for KDM6B (JMJD3) was performed essentially as described for KDM4A (JMJD2A) with the following modifications: A solution of 50 nM catalytic domain JMJD3 1043-end (BPS BioScience, San Diego, CA, USA) was used with 400 nM of biotinylated H3K27me$_3$ 21–44 substrate peptide ATKAARK(me$_3$)-SAPATGGVKKPHRYRPG-GK(biotin) (PSL Peptide Specialty Laboratories, Heidelberg, Germany). Incubation time for the enzymatic reaction was 120 min and the detection mix contained the appropriate europium-labeled anti-H3K27me$_2$ LANCE antibody (PerkinElmer).

KDM4A 2-oxoglutarate competition assay. To assess the competitive degree of enzyme inhibition by test compounds to 2-oxoglutarate, the LANCE*Ultra* assay was performed as described above with varying concentrations of 2-oxoglutarate (0–5.0 μM) and inhibitor (0–2.5 μM). Each combination was tested in duplicate. The blank-cor-

rected LANCE signal was compared with a pre-established calibration curve to determine the amount of demethylated product formed and, thus, the reaction velocity over the incubation time. Curve fitting was performed using the Michaelis–Menten equation:

$$v = \frac{v_{max} \cdot [\text{2-oxoglutarate}]}{K_M + [\text{2-oxoglutarate}]} \quad (1)$$

The apparent K_M values were plotted against the concentration of inhibitor to obtain K_i by linear regression to the equation:

$$K_M^{app} = K_M^0 \left(1 + \frac{[\text{compound}]}{K_i}\right) \quad (2)$$

Acknowledgements

M.J. and R.S. thank the Deutsche Forschungsgemeinschaft for funding (SFB992 MEDEP—Medical Epigenetics). M.R. thanks the Studienstiftung des deutschen Volkes for support. Furthermore, we thank Johanna Senger (University of Freiburg) for performing the histone deacetylase assay.

Keywords: acyl hydrazides · acyl hydrazones · epigenetics · histone demethylase · tetrazoles

[1] S. Krishnan, E. Collazo, P. A. Ortiz-Tello, R. C. Trievel, *Anal. Biochem.* **2012**, *420*, 48 – 53.
[2] C. Loenarz, C. J. Schofield, *Nat. Chem. Biol.* **2008**, *4*, 152 – 156.
[3] M. Kogure, M. Takawa, H. S. Cho, G. Toyokawa, K. Hayashi, T. Tsunoda, T. Kobayashi, Y. Daigo, M. Sugiyama, Y. Atomi, Y. Nakamura, R. Hamamoto, *Cancer Lett.* **2013**, *336*, 76 – 84.
[4] T. D. Kim, S. Shin, W. L. Berry, S. Oh, R. Janknecht, *J. Cell. Biochem.* **2012**, *113*, 1368 – 1376.
[5] a) W. Xu, K. Jiang, M. Shen, Y. Qian, Y. Peng, *Biol. Chem.* **2015**, *396*, 929 – 936; b) F. A. Mallette, S. Richard, *Cell Rep.* **2012**, *2*, 1233 – 1243.
[6] S. Shin, R. Janknecht, *Biochem. Biophys. Res. Commun.* **2007**, *359*, 742 – 746.
[7] a) W. L. Berry, S. Shin, S. A. Lightfoot, R. Janknecht, *Int. J. Oncol.* **2012**, *41*, 1701 – 1706; b) B. X. Li, M. C. Zhang, C. L. Luo, P. Yang, H. Li, H. M. Xu, H. F. Xu, Y. W. Shen, A. M. Xue, Z. Q. Zhao, *J. Exp. Clin. Cancer Res.* **2011**, *30*, 90.
[8] N. Patani, W. G. Jiang, R. F. Newbold, K. Mokbel, *Anticancer Res.* **2011**, *31*, 4115 – 4125.
[9] I. Hoffmann, M. Roatsch, M. L. Schmitt, L. Carlino, M. Pippel, W. Sippl, M. Jung, *Mol. Oncol.* **2012**, *6*, 683 – 703.
[10] E. C. Kauffman, B. D. Robinson, M. J. Downes, L. G. Powell, M. M. Lee, D. S. Scherr, L. J. Gudas, N. P. Mongan, *Mol. Carcinog.* **2011**, *50*, 931 – 944.
[11] L. Guerra-Calderas, R. González-Barrios, L. A. Herrera, D. Cantú de León, E. Soto-Reyes, *Cancer Genet.* **2015**, *208*, 215 – 224.
[12] C. Van Rechem, J. C. Black, P. Greninger, Y. Zhao, C. Donado, P. d. Burrowes, B. Ladd, D. C. Christiani, C. H. Benes, J. R. Whetstine, *Cancer Discovery* **2015**, *5*, 245 – 254.
[13] S. S. Ng, K. L. Kavanagh, M. A. McDonough, D. Butler, E. S. Pilka, B. M. R. Lienard, J. E. Bray, P. Savitsky, O. Gileadi, F. von Delft, N. R. Rose, J. Offer, J. C. Scheinost, T. Borowski, M. Sundstrom, C. J. Schofield, U. Oppermann, *Nature* **2007**, *448*, 87 – 91.
[14] J. C. Black, A. L. Manning, C. Van Rechem, J. Kim, B. Ladd, J. Cho, C. M. Pineda, N. Murphy, D. L. Daniels, C. Montagna, P. W. Lewis, K. Glass, C. D. Allis, N. J. Dyson, G. Getz, J. R. Whetstine, *Cell* **2013**, *154*, 541 – 555.
[15] Z. Z. Chen, J. Y. Zang, J. Whetstine, X. Hong, F. Davrazou, T. G. Kutateladze, M. Simpson, Q. L. Mao, C. H. Pan, S. D. Dai, J. Hagman, K. Hansen, Y. Shi, G. Y. Zhang, *Cell* **2006**, *125*, 691 – 702.
[16] E. C. Y. Woon, A. Tumber, A. Kawamura, L. Hillringhaus, W. Ge, N. R. Rose, J. H. Y. Ma, M. C. Chan, L. J. Walport, K. H. Che, S. S. Ng, B. D. Marsden, U. Oppermann, M. A. McDonough, C. J. Schofield, *Angew. Chem. Int. Ed.* **2012**, *51*, 1631 – 1634; *Angew. Chem.* **2012**, *124*, 1663 – 1666.
[17] a) R. J. Klose, K. Yamane, Y. J. Bae, D. Z. Zhang, H. Erdjument-Bromage, P. Tempst, J. M. Wong, Y. Zhang, *Nature* **2006**, *442*, 312 – 316; b) J. F. Couture, E. Collazo, P. A. Ortiz-Tello, J. S. Brunzelle, R. C. Trievel, *Nat. Struct. Mol. Biol.* **2007**, *14*, 689 – 695.
[18] J. R. Whetstine, A. Nottke, F. Lan, M. Huarte, S. Smolikov, Z. Z. Chen, E. Spooner, E. Li, G. Y. Zhang, M. Colaiacovo, Y. Shi, *Cell* **2006**, *125*, 467 – 481.
[19] M. Mantri, T. Krojer, E. A. Bagg, C. J. Webby, D. S. Butler, G. Kochan, K. L. Kavanagh, U. Oppermann, M. A. McDonough, C. J. Schofield, *J. Mol. Biol.* **2010**, *401*, 211 – 222.
[20] N. R. Rose, E. C. Y. Woon, A. Tumber, L. J. Walport, R. Chowdhury, X. S. Li, O. N. F. King, C. Lejeune, S. S. Ng, T. Krojer, M. C. Chan, A. M. Rydzik, R. J. Hopkinson, K. H. Che, M. Daniel, C. Strain-Damerell, C. Gileadi, G. Kochan, I. K. H. Leung, J. Dunford, K. K. Yeoh, P. J. Ratcliffe, N. Burgess-Brown, F. von Delft, S. Muller, B. Marsden, P. E. Brennan, M. A. McDonough, U. Oppermann, R. J. Klose, C. J. Schofield, A. Kawamura, *J. Med. Chem.* **2012**, *55*, 6639 – 6643.
[21] O. N. F. King, X. S. Li, M. Sakurai, A. Kawamura, N. R. Rose, S. S. Ng, A. M. Quinn, G. Rai, B. T. Mott, P. Beswick, R. J. Klose, U. Oppermann, A. Jadhav, T. D. Heightman, D. J. Maloney, C. J. Schofield, A. Simeonov, *PLoS One* **2010**, *5*, e15535.
[22] N. R. Rose, S. S. Ng, J. Mecinović, B. t. M. R. Liénard, S. H. Bello, Z. Sun, M. A. McDonough, U. Oppermann, C. J. Schofield, *J. Med. Chem.* **2008**, *51*, 7053 – 7056.
[23] S. Hamada, T. Suzuki, K. Mino, K. Kosek, F. Oehme, I. Flamme, H. Ozasa, Y. Itoh, D. Ogasawara, H. Komaarashi, A. Kato, H. Tsumoto, H. Nakagawa, M. Hasegawa, R. Sasaki, T. Mizukami, N. Miyata, *J. Med. Chem.* **2010**, *53*, 5629 – 5638.
[24] L. Wang, J. J. Chang, D. Varghese, M. Dellinger, S. Kumar, A. M. Best, J. Ruiz, R. Bruick, S. Pena-Llopis, J. J. Xu, D. J. Babinski, D. E. Frantz, R. A. Brekken, A. M. Quinn, A. Simeonov, J. Easmon, E. D. Martinez, *Nat. Commun.* **2013**, *4*, 2035.
[25] C. C. Thinnes, K. S. England, A. Kawamura, R. Chowdhury, C. J. Schofield, R. J. Hopkinson, *Biochim. Biophys. Acta Gene Regul. Mech.* **2014**, *1839*, 1416 – 1432.
[26] N. R. Rose, E. C. Y. Woon, G. L. Kingham, O. N. F. King, J. Mecinovic, I. J. Clifton, S. S. Ng, J. Talib-Hardy, U. Oppermann, M. A. McDonough, C. J. Schofield, *J. Med. Chem.* **2010**, *53*, 1810 – 1818.
[27] C. Hansch, A. Leo, *Exploring QSAR: Fundamentals and Applications in Chemistry and Biology, Vol. 1*, American Chemical Society, Washington, DC, **1995**.
[28] L. Friedman, H. Shechter, *J. Org. Chem.* **1960**, *25*, 877 – 879.
[29] W. G. Finnegan, R. A. Henry, R. Lofquist, *J. Am. Chem. Soc.* **1958**, *80*, 3908 – 3911.
[30] W. Schulze, *J. Prakt. Chem.* **1963**, *19*, 91 – 100.
[31] F. T. Luo, A. Jeevanandam, *Tetrahedron Lett.* **1998**, *39*, 9455 – 9456.
[32] T. Rabini, G. Vita, *J. Org. Chem.* **1965**, *30*, 2486 – 2488.
[33] H. Ulrich, J. N. Tilley, A. A. Sayigh, *J. Org. Chem.* **1962**, *27*, 2160 – 2162.
[34] R. Sekirnik, N. R. Rose, A. Thalhammer, P. T. Seden, J. Mecinović, C. J. Schofield, *Chem. Commun.* **2009**, 6376 – 6378.
[35] R. J. Hopkinson, A. Tumber, C. Yapp, R. Chowdhury, W. Aik, K. H. Che, X. S. Li, J. B. L. Kristensen, O. N. F. King, M. C. Chan, K. K. Yeoh, H. Choi, L. J. Walport, C. C. Thinnes, J. T. Bush, C. Lejeune, A. M. Rydzik, N. R. Rose, E. A. Bagg, M. A. McDonough, T. J. Krojer, W. W. Yue, S. S. Ng, L. Olsen, P. E. Brennan, U. Oppermann, S. Müller, R. J. Klose, P. J. Ratcliffe, C. J. Schofield, A. Kawamura, *Chem. Sci.* **2013**, *4*, 3110 – 3117.
[36] L. Kruidenier, C.-w. Chung, Z. Cheng, J. Liddle, K. Che, G. Joberty, M. Bantscheff, C. Bountra, A. Bridges, H. Diallo, D. Eberhard, S. Hutchinson, E. Jones, R. Katso, M. Leveridge, P. K. Mander, J. Mosley, C. Ramirez-Molina, P. Rowland, C. J. Schofield, R. J. Sheppard, J. E. Smith, C. Swales, R. Tanner, P. Thomas, A. Tumber, G. Drewes, U. Oppermann, D. J. Patel, K. Lee, D. M. Wilson, *Nature* **2012**, *488*, 404 – 408.
[37] B. Heinemann, J. M. Nielsen, H. R. Hudlebusch, M. J. Lees, D. V. Larsen, T. Boesen, M. Labelle, L.-O. Gerlach, P. Birk, K. Helin, *Nature* **2014**, *514*, E1 – E2.
[38] B. Heltweg, J. Trapp, M. Jung, *Methods* **2005**, *36*, 332 – 337.
[39] F. Wilde, A. Link, *Expert Opin. Drug Discovery* **2013**, *8*, 597 – 606.
[40] a) K.-H. Chang, O. N. F. King, A. Tumber, E. C. Y. Woon, T. D. Heightman, M. A. McDonough, C. J. Schofield, N. R. Rose, *ChemMedChem* **2011**, *6*,

759 – 764; b) R. Chowdhury, K. K. Yeoh, Y. M. Tian, L. Hillringhaus, E. A. Bagg, N. R. Rose, I. K. H. Leung, X. S. Li, E. C. Y. Woon, M. Yang, M. A. McDonough, O. N. King, I. J. Clifton, R. J. Klose, T. D. W. Claridge, P. J. Ratcliffe, C. J. Schofield, A. Kawamura, *EMBO Rep.* **2011**, *12*, 463 – 469; c) Z. Chen, J. Zang, J. Kappler, X. Hong, F. Crawford, Q. Wang, F. Lan, C. Jiang, J. Whetstine, S. Dai, K. Hansen, Y. Shi, G. Zhang, *Proc. Natl. Acad. Sci. USA* **2007**, *104*, 10818 – 10823.

[41] J. A. Day, S. M. Cohen, *J. Med. Chem.* **2013**, *56*, 7997 – 8007.

[42] A. C. Wallace, R. A. Laskowski, J. M. Thornton, *Prot. Eng. Des. Sel.* **1995**, *8*, 127 – 134.

Received: July 28, 2015
Published online on September 4, 2015